

# The cytoplasmic tail of NSP4, the endoplasmic reticulum-localized non-structural glycoprotein of rotavirus, contains distinct virus binding and coiled coil domains

John A. Taylor<sup>1</sup>, Judith A. O'Brien and Mark Yeager<sup>1,2</sup>

Biochemistry and Molecular Biology, School of Biological Sciences, University of Auckland, Private Bag 92019, Auckland, New Zealand and <sup>2</sup>The Scripps Research Institute, Department of Cell Biology, MB4a, 10666 North Torrey Pines Road, La Jolla, CA 92037, USA

<sup>1</sup>Corresponding authors

**The final steps in the assembly of rotavirus occur in the lumen of the endoplasmic reticulum (ER). Targeting of the immature inner capsid particle (ICP) to this compartment is mediated by the cytoplasmic tail of NSP4, a non-structural virus glycoprotein located in the ER membrane. To delineate structural and functional features of NSP4, soluble fragments of the cytoplasmic tail have been expressed and purified. Our analysis combines a functional assay for ICP binding with biochemical and CD spectroscopic studies to examine the secondary and quaternary structure. The ICP-binding domain is located within the C-terminal 20 amino acids of the polypeptide. A second region, distinct from this receptor domain, adopts an  $\alpha$ -helical coiled coil structure and mediates the oligomerization of the virus binding domains into a homotetramer. The domain organization of the cytoplasmic fragments of NSP4 suggests a novel structure for an icosahedral virus receptor protein in which C-terminal binding sites for immature rotavirus particles are connected to an  $\alpha$ -helical coiled coil stalk which projects from the ER membrane.**

**Keywords:**  $\alpha$ -helical coiled coil/CD spectroscopy/cytoplasmic tail/glycoprotein receptor/rotavirus assembly

## Introduction

Release of several enveloped viruses from infected cells is thought to proceed via a budding mechanism driven by multiple interactions between a ribonucleoprotein particle and the cytoplasmic tails of viral glycoproteins located in the plasma membrane (Simons and Garoff, 1980). Budding of rotavirus, a non-enveloped icosahedral virus, has also been proposed to occur during the assembly of mature virions. This budding event occurs across the endoplasmic reticulum (ER) membrane, and the final assembly of infectious particles takes place in the ER lumen. Members of several enveloped virus families, including flaviviruses and hepadnaviruses, share the ER as a site of intracellular maturation (Patzer *et al.*, 1986; Chambers *et al.*, 1990). However, rotavirus is unique in that the ER bilayer is only transiently associated with the budding rotavirus particle, which remains non-enveloped after transfer to the lumen. Electron microscopic analyses of infected cells have revealed that immature inner capsid particles (ICPs)

assemble in the viroplasm adjacent to the ER (Bellamy and Both, 1990). The ICP contains 11 double-stranded RNA segments and structural proteins VP1, VP2, VP3 and VP6. Budding of the ICP into the ER lumen is mediated by the cytoplasmic tail of a virally encoded 28 kDa, non-structural glycoprotein termed NSP4 (formerly NS28). The progressive envelopment of the ICP, driven by its interaction with NSP4, results in a transiently enveloped particle visible in electron micrographs of rotavirus-infected cells (Poruchynsky *et al.*, 1991). Infectious virions are subsequently formed by the assembly of an outer capsid layer containing VP7 and the VP4 hemagglutinin spike. The mechanism by which the ICP loses its transient envelope and NSP4 but selectively retains VP7 and VP4 is poorly understood. However, it is known that depletion of cellular  $\text{Ca}^{2+}$  or prevention of NSP4 glycosylation by tunicamycin treatment causes accumulation of enveloped particles within the ER and retention of NSP4 in the virion-associated envelope (Sabara *et al.*, 1982; Petrie *et al.*, 1983; Poruchynsky *et al.*, 1991). Although NSP4 is thought to form hetero-oligomeric complexes with VP7 and VP4, it is not a component of the mature infectious particle (Maass and Atkinson, 1990).

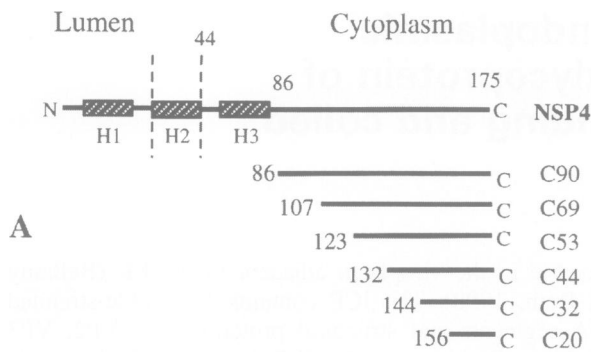
Topological analysis of NSP4 has revealed the presence of a single transmembrane domain, two glycosylation sites within a short luminal domain and a larger cytoplasmic tail (Figure 1A). Given its location on intracellular membranes, NSP4 represents a unique type of 'receptor' for an icosahedral virus particle and is functionally analogous to the membrane glycoproteins of enveloped viruses. In contrast to the latter group, many of the glycoproteins which mediate budding of enveloped viruses at the plasma membrane contain a relatively short cytoplasmic tail, with most of the polypeptide mass generally found on the extracellular face.

To delineate structural and functional features of the cytoplasmic tail of NSP4, soluble fragments of this region have been expressed and purified. Our analysis combines a functional assay for ICP binding with biochemical and CD spectroscopic studies to examine the secondary and quaternary structure. Our results suggest the presence of distinct viral binding and coiled coil domains within the cytoplasmic tail of NSP4, which represents a novel structural motif amongst proteins known to interact with icosahedral viruses.

## Results

### **Identification of an ICP receptor domain within the cytoplasmic tail of NSP4**

Previous work has implicated the importance of the C-terminus of NSP4 in the binding of the rotavirus ICP (Au *et al.*, 1989, 1993; Taylor *et al.*, 1992, 1993). However,



A

B

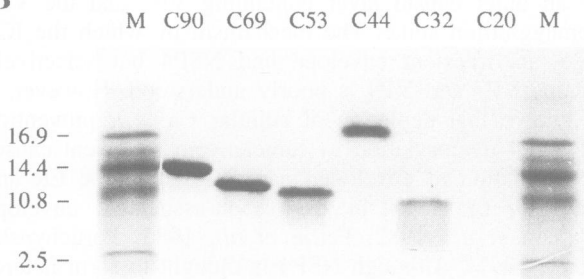


**Fig. 1.** (A) Schematic representation of the rotavirus intracellular receptor NSP4 and the series of six truncated soluble domains generated after thrombin cleavage of the respective GST fusion proteins. Each variant is designated by the number of amino acids retained from the C-terminal region of the protein. Shaded boxes represent hydrophobic domains within the full-length sequence. The dashed lines demarcate the ER bilayer. The proposed topology for NSP4 is from Bergmann *et al.* (1989). (B) SDS-PAGE analysis of the purified NSP4 domains. Aliquots of 10 µg of each truncated protein were visualized by Coomassie staining following electrophoresis. C44 migrated anomalously, presumably due to its higher net negative charge. C20 could not be visualized in stained gels using this technique. The sizes for the molecular weight markers (M) are indicated in kDa.

a minimum region of the cytoplasmic tail to which this receptor function can be assigned has not been defined. We therefore constructed a series of vectors designed to express progressively smaller portions of the C-terminus of NSP4 as fusions with glutathione *S*-transferase (GST) (Figure 1A). Fusion proteins were expressed in *Escherichia coli* and purified by affinity and gel filtration chromatography. The receptor activity of each recombinant protein was examined by measuring the binding of radiolabelled ICPs to GST fusion proteins immobilized on glutathione-Sepharose beads with the cytoplasmic receptor domain presented on the surface (Taylor *et al.*, 1993). Each variant exhibited comparable levels of ICP binding activity, indicating that the binding site for the particle must reside within the shortest variant, a 20 amino acid domain from the extreme C-terminus of NSP4 (Figure 2). The specificity of this interaction was demonstrated by the lack of ICP binding by: (i) immobilized GST alone and (ii) a mutant

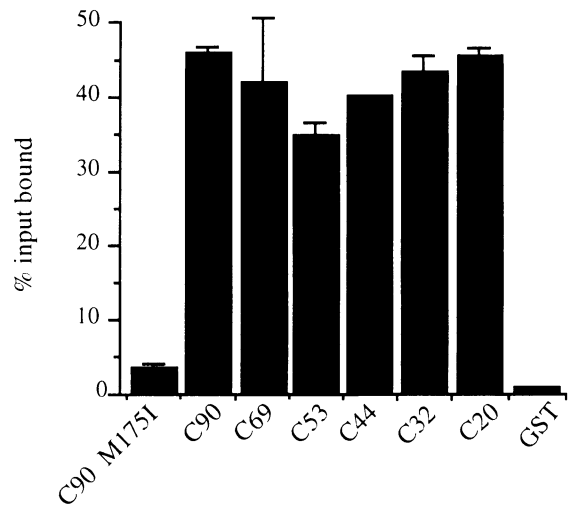


**Fig. 2.** Receptor binding assay using Sepharose bead-bound GST-NSP4 fusion proteins according to Taylor *et al.* (1993). All the truncated fusion proteins display comparable ICP binding ability except the point mutant M175I of C90, which has been included as a negative control (standard deviation is indicated).

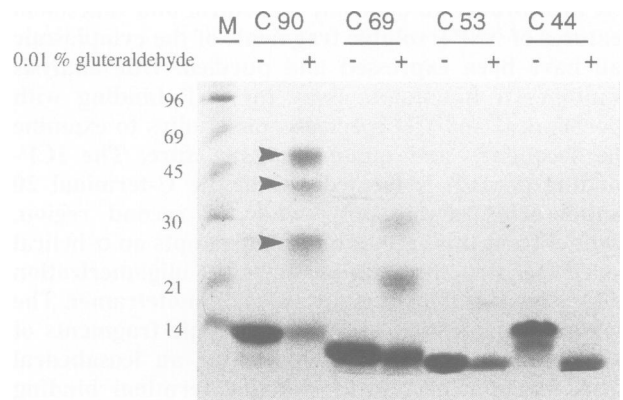


**Fig. 3.** Oligomeric state of the truncated receptors examined by glutaraldehyde cross-linking. Arrowheads indicate the inferred positions of dimeric, trimeric and tetrameric forms of C90. The anomalous migration of C44 is inhibited by the cross-linking reaction, causing it to migrate ahead of the non-cross-linked form.

form of C90 with a Met→Ile mutation at the extreme C-terminus, previously shown to abrogate ICP binding (Taylor *et al.*, 1993).

### Oligomeric state of the truncated receptor domains

Previous analysis of the longest cytoplasmic tail variant C90 revealed a putative homotetrameric structure (Taylor *et al.*, 1993). We therefore sought to analyze the quaternary structure of the remaining variants in order to define the domain(s) within the cytoplasmic tail that mediates oligomerization. The presence of oligomeric forms of each fragment of the cytoplasmic tail was investigated by cross-linking with glutaraldehyde, a bifunctional reagent, prior to analysis by SDS-PAGE. Cross-linking of C90 resulted in the presence of several higher molecular weight bands whose sizes correspond to dimeric, trimeric and tetrameric forms. Under identical reaction conditions, the majority of C69 remained in the monomeric form, and only a small fraction of the protein migrated as an oligomer (Figure 3). Cross-linking of C53 and C44 did not result in the

detection of any oligomeric forms, implying that these variants are exclusively monomeric. By extrapolation, we infer that the two shortest fragments, C34 and C20, are also monomeric. (The difficulty in detecting these species by SDS-PAGE analysis precluded cross-linking experiments.)

Differences in the quaternary structure of C90 and C69 were further examined by size exclusion chromatography (Figure 4). Comparison of the elution profile of each sample with a series of proteins of known mass revealed significant differences in the apparent molecular weights in solution. C90 was eluted as a single major peak with an apparent molecular weight of ~58 kDa, a value larger than expected for a tetramer with a subunit molecular weight of 10.8 kDa. This discrepancy may be accounted for by an extended conformation, rather than the globular structure exhibited by the standard proteins (Lau *et al.*, 1984). For instance, the calculated anhydrous Stoke's radius for C90 was 32.5 Å, which yields an estimated axial ratio of 7.2 for a prolate ellipsoid model for a C90 tetramer. In contrast, C69 also eluted as a single major peak with an apparent molecular weight of ~22 kDa. Since the calculated subunit molecular weight for C69 is 8.5 kDa, a value of ~22 kDa is inconsistent with a tetrameric structure, but may reflect the existence of a dimeric form in solution. Taken together, the results of the cross-linking studies and size exclusion chromatography suggest that only the longest fragment of the NSP4 cytoplasmic tail retains the ability to form a homotetramer in solution. Truncation of amino acids from the N-terminal end of this molecule results in the failure of the resultant species to oligomerize as a tetramer.

#### Correlation of $\alpha$ -helical content with the oligomeric state of the truncated proteins

The previous results suggest that a domain located within the N-terminal portion of C90 mediates oligomerization of this molecule into a tetramer. A possible conformation adopted by this region is suggested by the presence of a repeating heptad motif in which residues *a* and *d* of a seven residue sequence  $(abcdefg)_n$  are predominantly hydrophobic (Figure 5A). This sequence motif is characteristic of domains that assume  $\alpha$ -helical coiled coil structures and thereby mediate subunit oligomerization in a wide range of proteins (Cohen and Parry, 1986). Notably, the amino acid sequence within the putative coiled coil region of NSP4 from strain SA11 is identical to the analogous region of NSP4 from both a human and a bovine strain (data not shown). Indeed, this region of NSP4 exhibits sequence similarity with several fibrous proteins, such as keratins and myosin, known to contain extended  $\alpha$ -helical coiled coils (Mattion *et al.*, 1994). We therefore used CD spectroscopy to test the prediction that an  $\alpha$ -helical region of the receptor might be required for subunit association.

Under physiological conditions the CD spectrum of C90 suggests a significant fraction of  $\alpha$ -helicity based on the double minima at 222 and 208 nm, with a quantitative estimation of 22% (Figure 6). In contrast to C90, the CD spectrum for C69 shows only a shallow minimum at 222 nm and a deeper minimum at ~200 nm. These changes suggest a marked reduction in  $\alpha$ -helical content (from 22 to ~1.7%) and a corresponding increase in the proportion of polypeptide in  $\beta$ -sheet,  $\beta$ -turn and random conforma-

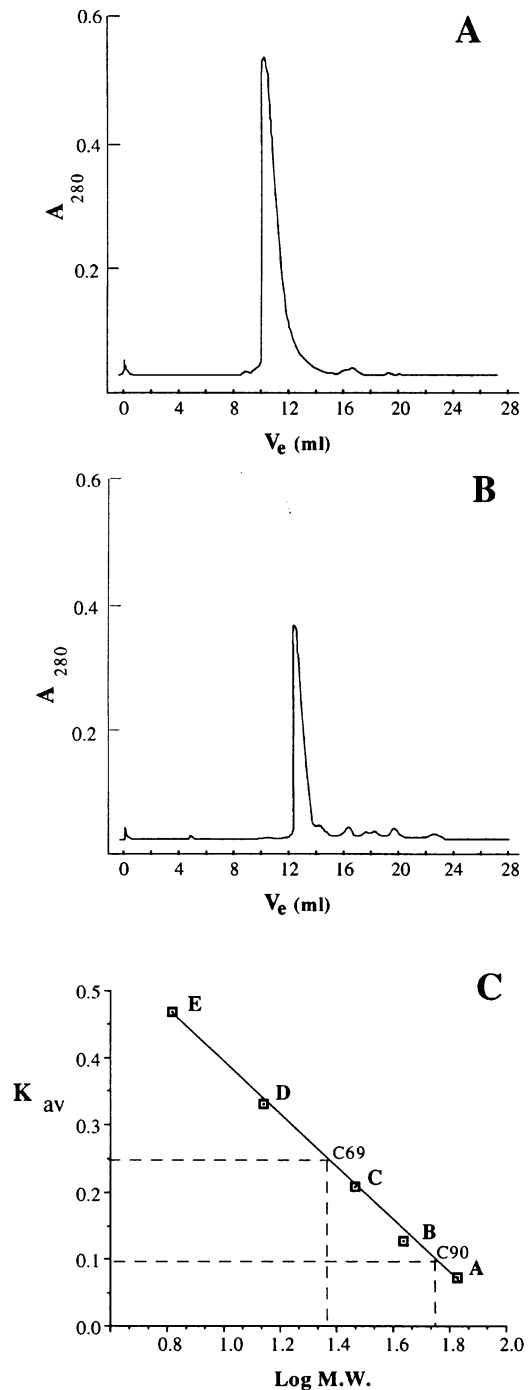


**Fig. 4.** Analysis of (A) C90 and (B) C69 by size exclusion chromatography as described in Materials and methods. (C) Calibration of the column with standard proteins and determination of apparent molecular weights of C69 and C90. A, bovine serum albumin, 67 kDa; B, ovalbumin, 45 kDa; C, carbonic anhydrase, 29 kDa; D, RNase A, 13.7 kDa; E, aproptinin, 6.5 kDa.

tions. CD analysis of each of the successively truncated receptors shows a virtual absence of  $\alpha$ -helical content and roughly equal proportions of  $\beta$ -sheet,  $\beta$ -turn and random conformations. These results suggest that a region of  $\alpha$ -helix is present in that variant of the soluble receptor that retains amino acids 86–106 and which, by inference, consequently assumes a tetrameric structure.

Since coiled coils are stabilized by non-covalent inter-

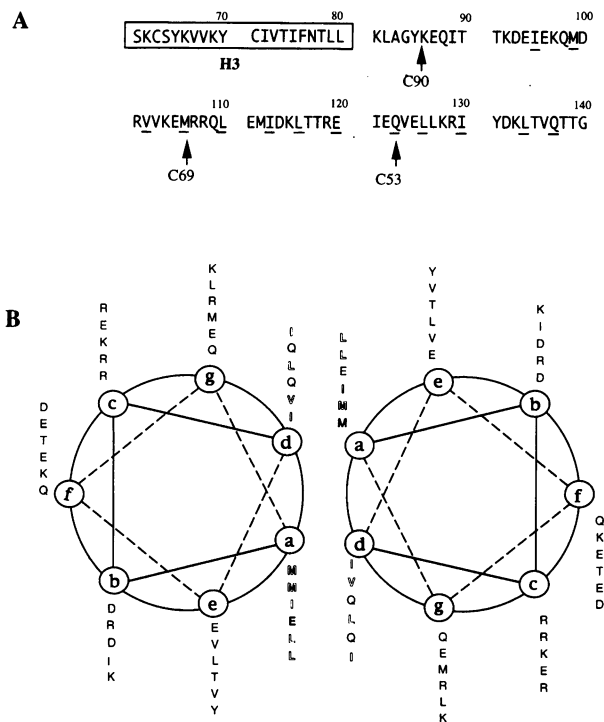


**Fig. 5.** A proposed  $\alpha$ -helical coiled coil domain within the cytoplasmic region of NSP4. (A) Amino acid sequence of the region of NSP4 (SA11 strain) that spans the hydrophobic region H3 (boxed) and the putative coiled coil domain (residues 95–137). The first residue of the truncated proteins C90, C69 and C53 is indicated. Underlined residues are those at positions *a* and *d* within each heptad (*abcdefg*)<sub>n</sub>. The first complete heptad begins at Met99. (B) Helical wheel projections of two NSP4 subunits showing the distribution of residues in the putative  $\alpha$ -helical region. Non-polar residues at heptad positions *a* and *d* are in outline typeface.

actions between subunits, a loss of  $\alpha$ -helicity should accompany disassociation of the constituent monomers. Hence, we examined the thermal stability of C90. The sigmoid melting curve (Figure 7A) demonstrates a single reversible thermal transition, consistent with an  $\alpha$ -helical coiled coil. The melting temperature ( $T_m$ ) increased with sample concentration (Figure 7B), consistent with stabilization of helicity by the self-association of monomers (O'Shea *et al.*, 1989). In summary, these data support a model in which the oligomerization of the cytoplasmic tail of NSP4 is mediated by an  $\alpha$ -helical coiled coil consisting of four subunits intertwined in a superhelical fiber.

**Limited proteolysis removes the ICP binding domain from the cytoplasmic tail**

Secondary structure analysis of the truncated receptor proteins suggests that the N-terminal region of the cytoplasmic domain assumes a highly ordered  $\alpha$ -helical conformation, whereas the C-terminal region has a high proportion of random,  $\beta$ -sheet and  $\beta$ -turn conformations. We reasoned that such a conformation might render the C-terminal region sensitive to proteolytic enzymes. We therefore used trypsin digestion to further probe the conformation of C90 (Figure 8). The results indicate the presence of one or more trypsin-sensitive sites within C90. After a 2 min incubation, virtually all the protein was converted to a shorter form which migrated with an

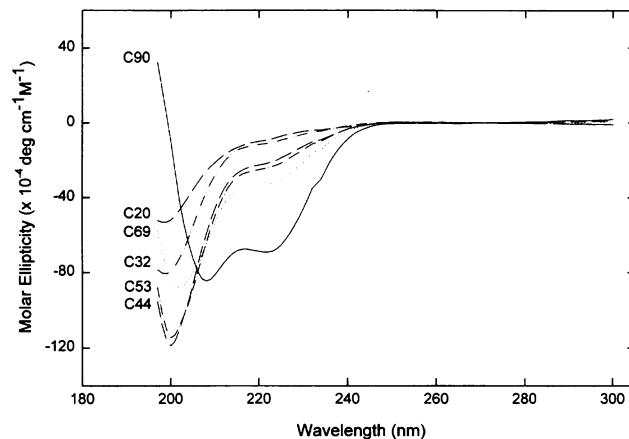


**Fig. 6.** CD spectra of the truncated NSP4 proteins. Only the spectrum for C90 exhibits minima at 222 and 208 nm that are characteristic of an  $\alpha$ -helical conformation. The monomer concentration of each sample was 50  $\mu$ M.

apparent molecular weight of  $\sim$ 9 kDa, and prolonged incubation resulted in the appearance of an additional proteolytic product (Figure 8A). N-Terminal sequence analysis of the digestion products (Figure 8B) confirmed that the N-termini of both polypeptides detectable by SDS-PAGE (designated P<sub>1</sub> and P<sub>2</sub>) were identical to that of the undigested protein. Since numerous potential trypsin cleavage sites are present throughout the length of C90 (Bergmann *et al.*, 1989), we conclude that only the C-terminal (receptor) region of the protein is accessible to trypsin cleavage, while the N-terminal region is trypsin-resistant. The close association of C90 subunits via their N-terminal regions presumably makes potential cleavage sites sterically inaccessible to added protease.

**Discussion**

Rotavirus morphogenesis is unique in that an icosahedral, immature particle assembles in the cytoplasm and subsequently buds across the ER membrane to acquire the outer capsid layer without the concomitant acquisition of a lipid envelope. Previous studies have revealed that transfer into the ER lumen is mediated by the cytoplasmic tail of the virally encoded, ER-localized, non-structural glycoprotein NSP4. In order to examine the structure and function of this intracellular receptor, we expressed and purified soluble polypeptides corresponding to various lengths of the cytoplasmic tail.

**Localization of the viral binding domain to the C-terminal 20 amino acids of NSP4**

A primary objective of this study was to determine the minimal region of the C-terminus required to mediate binding of the ICP. Previous analysis of a full-length NSP4 mutant expressed in mammalian cells demonstrated that substitution of the C-terminal methionine by isoleucine prevented ICP binding (Taylor *et al.*, 1992). Similar results were obtained for a soluble NSP4 variant containing the C-terminal 90 amino acids (C90) expressed in *E.coli* (Taylor *et al.*, 1993). Au *et al.* (1993) utilized an *in vitro* expression system to demonstrate that loss of residues 161–175 also prevented ICP binding. However, these workers found that a peptide corresponding to residues

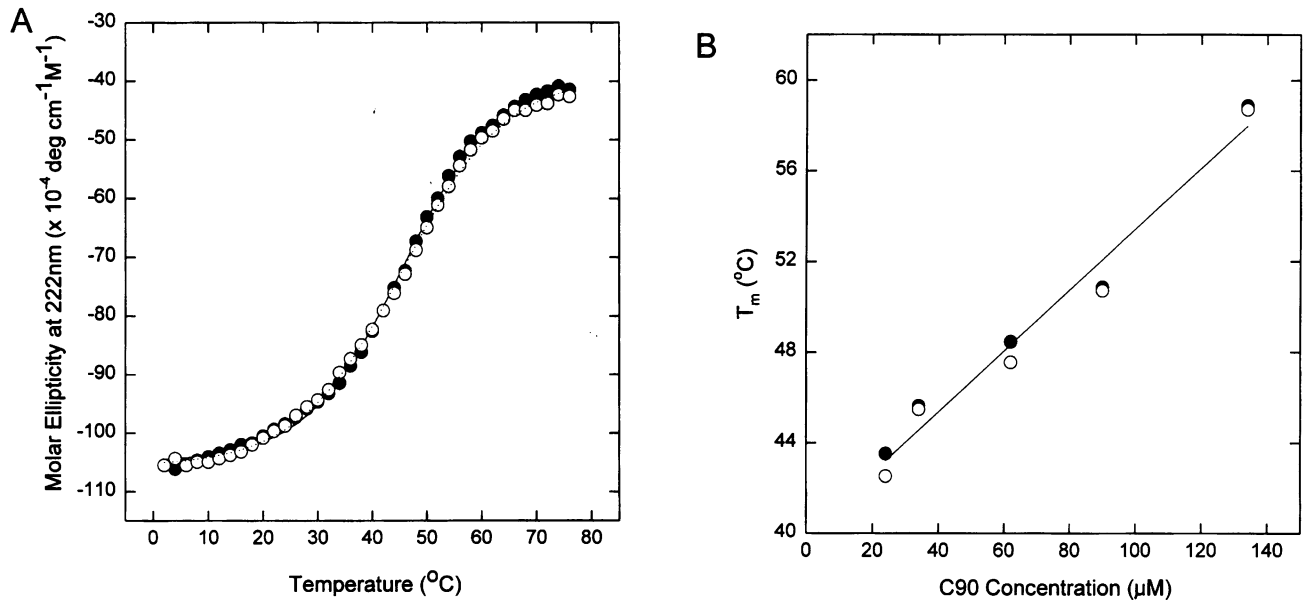


**Fig. 7.** (A) Temperature dependence of the  $\alpha$ -helical stability of C90. Heating (closed circles) and cooling (open circles) profiles display very little hysteresis. The monomer concentration was 34  $\mu\text{M}$ . (B) The melting temperature  $T_m$  (see equation 2) for a given sample concentration is linearly dependent on C90 concentration over the experimental range.

161–172 from NSP4 did not block binding of ICPs using a solid phase assay. In this study we have also utilized a solid phase assay in which truncated regions of the C-terminus of NSP4 were immobilized on Sepharose beads as GST fusion proteins. Our results demonstrate that only the C-terminal 20 amino acids are necessary for ICP binding, and the remainder of NSP4 can be deleted. (We cannot rule out the possibility that the minimal binding domain is smaller than the C-terminal 20 amino acids.) Surprisingly, no apparent benefit is derived by using a tetrameric form of the receptor over the 20 amino acid minimal binding domain in the solid phase assay. However, this may not reflect the *in vivo* requirements for ICP binding, where a tetrameric NSP4 molecule may enable cooperative binding of its C-terminal domains to the particle. It is noteworthy that the solid phase assay may involve multivalent binding of the NSP4 peptides to a single ICP. This may account for the inability of soluble peptides corresponding to amino acids 161–172 to block ICP binding (Au *et al.*, 1993). Indeed, the solid phase assay may mimic more closely the binding of ICPs to membrane-bound NSP4.

**An N-terminal coiled coil domain within the cytoplasmic tail mediates oligomerization of NSP4**

The second objective of this study was to examine the secondary and quaternary structure of NSP4. Previous cross-linking studies suggested that C90 may form oligomers (Taylor *et al.*, 1993). The availability of purified, truncated forms of the cytoplasmic tail allowed us to delineate the domain(s) responsible for subunit oligomerization and secondary structure. The cross-linking and gel filtration experiments described here confirm the existence of oligomeric forms of C90 and suggest that this polypeptide forms a homotetramer in solution. However, the failure of truncated forms of C90 to exhibit comparable oligomerization suggests that the N-terminal portion of C90 is primarily responsible for stability of the oligomers.

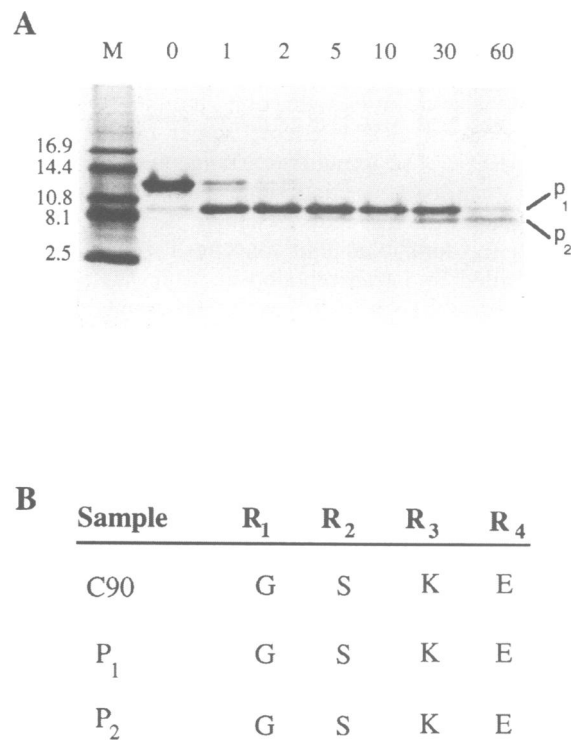


**Fig. 8.** (A) Time course (min) for the digestion of C90 by trypsin. P<sub>1</sub> and P<sub>2</sub> represent products of progressive trypsin digestion. Sizes (in kDa) for the molecular weight markers (M) are indicated. (B) N-Terminal sequence analysis of C90 and the trypsin degradation products P<sub>1</sub> and P<sub>2</sub>. The first four N-terminal residues were determined by the method of Matsudiara (1987).

This conclusion is supported by sequence analyses of NSP4, which reveal the presence of heptad repeats. This sequence motif is characteristic of domains that assume

$\alpha$ -helical coiled coil structures and thereby mediate subunit oligomerization in several proteins (Cohen and Parry, 1986). CD spectroscopy was utilized to test the prediction that a coiled coil motif mediates the oligomerization of C90. The CD spectrum of C90 clearly indicates the presence of  $\alpha$ -helical secondary structure that is absent from the truncated variants lacking part or all of the heptad-spanning region. The amount of  $\alpha$ -helical structure in C90, calculated at 22% from the CD data, was lower than expected. Given the presence of an uninterrupted heptad repeat corresponding to residues 95–137 in the native protein sequence (Figure 5), a value closer to 50% was anticipated. Furthermore, the  $\alpha$ -helical content of C69 was determined by CD to be <2%, despite the retention of the majority of the heptad-spanning region at the N-terminus of this variant. One explanation for this discrepancy could be that the region that is not common between C90 and C69 (residues 86–105) is solely responsible for tetramerization via coiled coil formation. Indeed, the relative mass of this domain is consistent with an  $\alpha$ -helical content of 22% for C90. However, a more likely scenario may be that this region could initiate the folding or be critical for the stability of helical structure, and its absence may prevent folding in C69 as is present in the intact protein.

The melting analysis displays a single cooperative and reversible unfolding of the  $\alpha$ -helical oligomer of NSP4, suggesting that the  $\alpha$ -helical conformation is stabilized by subunit association. These results are comparable with the melting behavior of two, three and four stranded  $\alpha$ -helical coiled coils in GCN4 leucine zipper mutants (Harbury *et al.*, 1993). The tetrameric arrangement of NSP4 may confer stability to the individual subunits. For instance, membrane proteins may assemble as multimers even though the functional unit may be a monomer. This is exemplified by bacteriorhodopsin, which assembles as a trimer even though each subunit functions as a proton pump (Henderson *et al.*, 1990), and the water channel protein CHIP28, which assembles as a tetramer even though each subunit functions as a selective water channel (Mitra *et al.*, 1995).

Based on crystallographic studies,  $\alpha$ -helical coiled coils are known to mediate subunit oligomerization in both dimeric and trimeric polypeptides (Wilson *et al.*, 1981; O'Shea *et al.*, 1989). Harbury *et al.* (1993) demonstrated that a peptide corresponding to a mutant form of the GCN4 leucine zipper region crystallized as a parallel four stranded  $\alpha$ -helical coiled coil. These authors correlated the distribution of  $\beta$ -branched amino acids within a given heptad with the number of subunits found in the resultant coiled coil. Accordingly, a preponderance of Ile and Val residues at position *d* of the heptad repeat found in NSP4 (Figure 5B) is in agreement with the prediction that this region of the protein folds as a tetrameric coiled coil. A high proportion of uncharged residues at the *g* and *e* positions is also consistent with the notion that these residues would be substantially buried within a tetrameric coiled coil. However, our experiments do not address the orientation of subunits within the putative coiled coil. The asymmetrical topology of NSP4 in the ER membrane (Figure 1A) would appear to necessitate a parallel orientation for the subunits. Confirmation of such a model for the cytoplasmic tail of NSP4 will require additional

spectroscopic as well as crystallographic analysis. Based on our current results, we nevertheless propose that the cytoplasmic tail of NSP4 contains at least two domains. ICP binding is mediated by a small protease-sensitive domain at the extreme C-terminus. A second domain, proximal to the ER membrane in the full-length protein, is proposed to mediate oligomerization via a coiled coil motif.

### **Comparison of NSP4 with glycoproteins that mediate budding of enveloped viruses**

Budding of alphaviruses at the plasma membrane has been shown to be dependent on interactions between the nucleocapsid and the cytoplasmic tail of transmembrane glycoproteins (Simons and Garoff, 1980; Suomalainen *et al.*, 1992). Using a solid phase assay, Metsikko and Garoff (1990) analyzed the binding of isolated nucleocapsid particles to synthetic peptides representing either the entire cytoplasmic tail of the E2 glycoprotein or a variant lacking a C-terminal domain. These studies revealed that binding of Semliki Forest virus (SFV) nucleocapsids was mediated by the C-terminal region of the cytoplasmic tail, a result similar to that reported here for ICP binding by NSP4. Moreover, the E2 cytoplasmic tail peptide formed oligomers in solution which the authors proposed might involve the association of the N-terminal regions. This arrangement of functional domains within the cytoplasmic tail of the SFV E2 glycoprotein is shared by NSP4.

Finally, it is noteworthy that the region of NSP4 shown here to adopt a coiled coil structure has recently been implicated in the NSP4-induced increase in intracellular calcium levels ( $[Ca^{2+}]_i$ ) observed during expression of this protein in insect cells (Tian *et al.*, 1995). It is not known, however, whether a peptide which maps to this region of NSP4 and causes elevated  $[Ca^{2+}]_i$  shares the conformation or multimeric state of the truncated form of the glycoprotein described here. The cytoplasmic tail of NSP4 may therefore play a key role in both viral assembly and pathogenesis during rotavirus infection.

## **Materials and methods**

### **Construction of GST-NSP4 fusion proteins**

Expression of a soluble, cytoplasmic domain of NSP4 (C90 =  $\Delta$ 1–85 NS28) as a GST fusion protein in *E.coli* has been described previously (Taylor *et al.*, 1993). Successively truncated regions of NSP4 cDNA were generated by PCR using a set of primers which introduced an *EcoRI* site at appropriate positions within the SA11 gene 10 cDNA. A common primer introduced an *EcoRI* site after the termination codon. The amplified and truncated cDNA fragments were cloned into the expression vector pGEX.2T (Amrad-Pharmacia Biotech, Melbourne, Australia). Constructs were confirmed by DNA sequencing using an Applied Biosystems automated sequencer. All fusion proteins (except GST-C90) were constructed so that thrombin cleavage of the fusion protein yielded a Gly-Ser-Pro-Gly-Ile sequence at the N-terminus of the soluble receptor.

### **Protein expression and purification**

Truncated cDNAs were expressed as GST fusion proteins in *E.coli* DH5 $\alpha$  (Smith and Johnson, 1988). After adsorption of fusion proteins to glutathione-Sepharose 4B (Amrad Pharmacia Biotech), the C90 and C69 domains were proteolytically removed by incubating the bead suspension with thrombin as previously described (Taylor *et al.*, 1993). The remaining smaller fusion proteins were eluted from the beads with 5 mM glutathione and dialyzed overnight against a buffer containing 25 mM Tris-HCl, pH 7.5, 10 mM NaCl and 2.5 mM CaCl<sub>2</sub>. Samples

were then concentrated further by ultrafiltration (Amicon 10) and cleaved with 10 U bovine thrombin (Sigma, St Louis, MO) per mg fusion protein at 37°C for 90 min in a 1 ml volume. Subsequent purification of each polypeptide employed gel filtration chromatography using a Superdex 75 column (Amrad Pharmacia Biotech) equilibrated with phosphate-buffered saline (PBS). The purity of each peptide was confirmed by SDS-PAGE (Schägger and von Jagow, 1987) and reverse phase HPLC. Protein concentration was measured using the BCA assay reagent (Pierce, Rockford, IL) or deduced from the absorbance of the single Trp residue in the presence of 6 M guanidine-HCl (Edelhoch, 1967).

#### Glutaraldehyde cross-linking of truncated receptors

Cross-linking reactions were performed as described by Jaenicke and Rudolph (1986). Protein samples (10 µg total) were diluted to a volume of 0.2 ml in PBS. Glutaraldehyde (EM grade) was added to a final concentration of 0.01%, and the samples were incubated at room temperature for 15 min. The reaction was quenched by the addition of 10 µl sodium borohydride (2 M in 0.1 M NaOH), and the samples were incubated for a further 20 min. Truncated proteins were precipitated by addition of ice-cold trichloroacetic acid to 7.5% and recovered by centrifugation. Pellets were resuspended in SDS sample buffer and analyzed by SDS-PAGE (Laemmli, 1970).

#### Analysis of truncated proteins by gel filtration chromatography

Gel filtration chromatography was performed on a Superdex 75 column connected to an FPLC system. The column was calibrated using proteins of known molecular weight (bovine serum albumin, 67 kDa; ovalbumin, 45 kDa; carbonic anhydrase, 28 kDa; RNase A, 13.4 kDa; aprotinin, 6.5 kDa), by plotting  $K_{av}$  versus log(molecular weight).

$$K_{av} = V_e - V_0/V_t - V_0 \quad (1)$$

where  $V_e$  is the elution volume of protein,  $V_0$  is the void volume of the column obtained from the elution of dextran blue and  $V_t$  is the column volume (24 ml). Aliquots (200 µl) of each truncated protein at a concentration of 100 µM (monomer) were injected onto the column, eluted with PBS, and the molecular weight value was calculated by comparison with the standard proteins. A plot of  $\sqrt{-\log(K_{av})}$  versus the Stoke's radius for each standard protein was used to determine the anhydrous Stoke's radius of C90. The anhydrous Stoke's radius ( $r$ ) of a protein is given by

$$r = (f/f_0)[(3/4\pi)(M\bar{v}/N_A)]^{1/3} \quad (2)$$

where  $f/f_0$  is the frictional coefficient,  $\bar{v}$  is the partial specific volume (assumed to be 0.73 cm<sup>3</sup>/g),  $M$  is the molecular weight (10 880×4 for a C90 tetramer) and  $N_A$  is Avogadro's constant (Winzor, 1969). Using these values,  $f/f_0$  for C90 is 1.4. The axial ratio of C90 was estimated from a plot of  $f/f_0$  for prolate ellipsoids (Van Holde, 1971).

#### Circular dichroism spectroscopy

Circular dichroism spectra were recorded from 50 µM (monomer) solutions of each truncated polypeptide in 10 mM sodium phosphate, pH 7.0, 150 mM NaCl. Samples were maintained at 4°C in a 1 mm path length quartz cell (Helma Kuvetten, Mulheim, Germany) using an AVIV spectropolarimeter. To monitor instrumental variation, 10 buffer scans were recorded before and after 15 sample scans over a wavelength range from 300 to 197 nm in increments of 0.2 nm. Absorption by NaCl precluded measurements below 197 nm. Analysis and processing of the data were as described by Cascio *et al.* (1990), with the buffer and sample scans being separately averaged, smoothed and then subtracted. Using characteristic basis spectra (Chang *et al.*, 1978), a non-linear least-squares curve fitting routine was used to determine the proportions of  $\alpha$ -helix,  $\beta$ -sheet,  $\beta$ -turn and random coil. Melting and annealing curves were generated by monitoring the ellipticity at 222 nm as the temperature was raised from 4 to 76°C and cooled to 4°C. The profiles were fitted using a four parameter logistic function model to describe a symmetrical sigmoid curve.

$$\theta_{222} = a/(1 + e^{b(T - T_m)}) + \theta_{min} \quad (3)$$

where  $\theta_{222}$  is the background subtracted ellipticity,  $T$  is the temperature,  $a$  is the range of ellipticity values,  $b$  is the slope coefficient,  $T_m$  is the temperature at the maximum rate of change of  $\theta_{222}$ , and  $\theta_{min}$  is the minimum ellipticity.

#### Trypsin digestion of C90

An aliquot of 10 µg C90 was incubated with 0.1 µg trypsin (TPCK-treated; Sigma, St Louis, MO) in 10 mM HEPES-KOH, pH 7.4, 100 mM NaCl and 2 mM CaCl<sub>2</sub>. Proteolysis was carried out at room temperature

and was terminated after the indicated time by the addition of 2 mM Pefabloc (Boehringer Mannheim, Mannheim, Germany). The products of digestion were analyzed by gel electrophoresis and Coomassie staining as described by Schägger and von Jagow (1987). Determination of the N-terminal sequence of C90 and the shorter trypsin-resistant forms was achieved following the method of Matsudaira (1987).

## Acknowledgements

We wish to thank Malcolm White for suggestions on sequence prediction, Catriona Knight for assistance with amino acid sequencing and Drs D.Maass, A.R.Bellamy, D.L.Christie and J.Kistler for critical reading of the manuscript. This work was supported by a Programme Grant from the Health Research Council of New Zealand awarded to A.R.Bellamy and a grant from the Auckland Medical Research Foundation to JAT. MY is an Established Investigator of the American Heart Association and Bristol-Myers Squibb and has been supported by the National Institutes of Health (RO1A131535 and RO1HL48908), a Grant-in-Aid from the American Heart Association National Center (92008120) and the Gustavus and Louise Pfeiffer Research Foundation.

## References

- Au,K.-S., Chan,W.-K., Burns,J.W. and Estes,M.K. (1989) Receptor activity of rotavirus nonstructural glycoprotein NS28. *J. Virol.*, **63**, 4553-4562.
- Au,K.-S., Mattion,N.M. and Estes,M.K. (1993) A subviral particle binding domain on the rotavirus nonstructural glycoprotein NS28. *Virology*, **194**, 665-673.
- Bellamy,A.R. and Both,G.W. (1990) Molecular biology of rotaviruses. *Adv. Virus Res.*, **38**, 1-43.
- Bergmann,C.C., Maass,D., Poruchynsky,M.S., Atkinson,P.H. and Bellamy,A.R. (1989) Topology of the non-structural rotavirus receptor glycoprotein NS28 in the rough endoplasmic reticulum. *EMBO J.*, **8**, 1695-1703.
- Cascio,M., Gogol,E. and Wallace,B.A. (1990) The secondary structure of gap junctions. Influence of isolation methods and proteolysis. *J. Biol. Chem.*, **265**, 2358-2364.
- Chambers,T.J., Hahn,C.S., Galler,R. and Rice,C.M. (1990) Flavivirus genome organization, expression, and replication. *Annu. Rev. Microbiol.*, **44**, 649-688.
- Chang,C.T., Wu,C.-S.C. and Yang,J.T. (1978) Circular dichroic analysis of protein conformation: inclusion of the  $\beta$ -turns. *Anal. Biochem.*, **91**, 13-31.
- Cohen,C. and Parry,D.A.D. (1986)  $\alpha$ -helical coiled coils—a widespread motif in proteins. *Trends Biochem. Sci.*, **11**, 245-248.
- Edelhoch,H. (1967) Spectroscopic determination of tryptophan and tyrosine in proteins. *Biochemistry*, **6**, 1948-1954.
- Harbury,P.B., Zhang,T., Kim,P.S. and Alber,T. (1993) A switch between two-, three-, and four-stranded coiled coils in GCN4 leucine zipper mutants. *Science*, **262**, 1401-1407.
- Henderson,R., Baldwin,J.M., Ceska,T.A., Zemlin,F., Beckmann,E. and Downing,K.H. (1990) Model for the structure of bacteriorhodopsin based on high-resolution electron cryo-microscopy. *J. Mol. Biol.*, **213**, 899-929.
- Jaenicke,R. and Rudolph,R. (1986) Refolding and association of oligomeric proteins. *Methods Enzymol.*, **131**, 218-250.
- Laemmli,U.K. (1970) Cleavage of structural proteins during the assembly of the head of bacteriophage T4. *Nature*, **227**, 680-685.
- Lau,S.Y.M., Taneja,A.K. and Hodges,R.S. (1984) Synthesis of a model protein of defined secondary and quaternary structure. Effect of chain length on the stabilization and formation of two-stranded  $\alpha$ -helical coiled-coils. *J. Biol. Chem.*, **259**, 13253-13261.
- Maass,D.R. and Atkinson,P.H. (1990) Rotavirus proteins VP7, NS28, and VP4 form oligomeric structures. *J. Virol.*, **64**, 2632-2641.
- Matsudaira,P. (1987) Sequence from picomole quantities of proteins electroblotted onto polyvinylidene difluoride membranes. *J. Biol. Chem.*, **262**, 10035-10038.
- Mattion,N.M., Cohen,J. and Estes,M.K. (1994) The rotavirus proteins. In Kapikian,A.Z. (ed.), *Viral Infections of the Gastrointestinal Tract*, 2nd edn. Marcel Dekker, New York, NY, pp. 169-250.
- Metsikkö,K. and Garoff,H. (1990) Oligomers of the cytoplasmic domain of the p62/E2 membrane protein of Semliki Forest virus bind to the nucleocapsid *in vitro*. *J. Virol.*, **64**, 4678-4683.

- Mitra,A.K., van Hoek,A.N., Wiener,M.C., Verkman,A.S. and Yeager,M. (1995) The CHIP28 water channel visualized in ice by electron crystallography. *Nature Struct. Biol.*, **2**, 726–729.
- O'Shea,E.K., Rutkowski,R. and Kim,P.S. (1989) Evidence that the leucine zipper is a coiled coil. *Science*, **243**, 538–542.
- Patzner,E.J., Nakamura,G.R., Simonsen,C.C., Levinson,A.D. and Brands,R. (1986) Intracellular assembly and packaging of Hepatitis B surface antigen particles occur in the endoplasmic reticulum. *J. Virol.*, **58**, 884–892.
- Petrie,B.L., Estes,M.K. and Graham,D.Y. (1983) Effects of tunicamycin on rotavirus morphogenesis and infectivity. *J. Virol.*, **46**, 270–274.
- Poruchynsky,M.S., Maass,D.R. and Atkinson,P.H. (1991) Calcium depletion blocks the maturation of rotavirus by altering the oligomerization of virus-encoded proteins in the ER. *J. Cell Biol.*, **114**, 651–661.
- Sabara,M., Babiuk,L.A., Gilchrist,J. and Misra,V. (1982) Effect of tunicamycin on rotavirus assembly and infectivity. *J. Virol.*, **43**, 1082–1090.
- Schägger,H. and von Jagow,G. (1987) Tricine–sodium dodecyl sulfate–polyacrylamide gel electrophoresis for the separation of proteins in the range from 1 to 100 kDa. *Anal. Biochem.*, **166**, 368–379.
- Simons,K. and Garoff,H. (1980) The budding mechanisms of enveloped animal viruses. *J. Gen. Virol.*, **50**, 1–21.
- Smith,D.B. and Johnson,K.S. (1988) Single-step purification of polypeptides expressed in *Escherichia coli* as fusions with glutathione S-transferase. *Gene*, **67**, 31–40.
- Suomalainen,M., Liljeström,P. and Garoff,H. (1992) Spike protein–nucleocapsid interactions drive the budding of alphaviruses. *J. Virol.*, **66**, 4737–4747.
- Taylor,J.A., Meyer,J.C., Legge,M.A., O'Brien,J.A., Street,J.E., Lord,V.J., Bergmann,C.C. and Bellamy,A.R. (1992) Transient expression and mutational analysis of the rotavirus intracellular receptor: the C-terminal methionine residue is essential for ligand binding. *J. Virol.*, **66**, 3566–3572.
- Taylor,J.A., O'Brien,J.A., Lord,V.J., Meyer,J.C. and Bellamy,A.R. (1993) The RER-localized rotavirus intracellular receptor: a truncated purified soluble form is multivalent and binds virus particles. *Virology*, **194**, 807–814.
- Tian,P., Estes,M.K., Hu,Y., Ball,J.M., Zeng,C.Q.-Y. and Schilling,W.P. (1995) The rotavirus nonstructural glycoprotein NSP4 mobilizes Ca<sup>2+</sup> from the endoplasmic reticulum. *J. Virol.*, **69**, 5763–5772.
- Van Holde,K.E. (1971) *Physical Biochemistry*. Prentice-Hall, Englewood Cliffs, NJ, p. 81.
- Wilson,I.A., Skehel,J.J. and Wiley,D.C. (1981) Structure of the haemagglutinin membrane glycoprotein of influenza virus at 3Å resolution. *Nature*, **289**, 366–373.
- Winzor,D.J. (1969) In Leach,S.J. (ed.), *Physical Principles and Techniques of Protein Chemistry—Part A*. Academic Press, New York, NY, p. 469.

Received on December 5, 1995; revised on May 7, 1996